

Bounds on non-standard interactions of neutrinos from IceCube DeepCore data

S. V. Demidov^{a,1},

^a*Institute for Nuclear Research of the Russian Academy of Sciences,
60th October Anniversary prospect 7a, Moscow 117312, Russia*

Abstract

New physics in neutrino sector can reveal itself via non-standard neutrino interactions which can result in modification of the standard picture of neutrino propagation in matter. Experiments with atmospheric neutrinos has been used to probe this scenario. Using publicly available three-year low energy data in IceCube DeepCore we place bounds on the parameters $\epsilon_{\alpha\beta}$ of non-standard neutrino interactions in propagation. We obtain restrictive constraints not only for $\mu\tau$ sector but also for flavor changing interactions involving electron neutrinos.

1 Introduction

Phenomenon of neutrino oscillations is well established by many experiments [1]. It implies nontrivial mixing between neutrinos and non-zero values of their masses. Explanation of these properties of neutrinos lies beyond the Standard Model and requires new physics. The latter may reveal itself via non-renormalizable interactions involving neutrino fields. In particular, new Fermi-type interactions of neutrinos with SM fermions are of interest and they are known as non-standard neutrino interactions [2,3]. In what follows we consider neutral current (NC) or matter non-standard neutrino interactions (NSI) with the lagrangian

$$\mathcal{L}_{NSI}^{NC} = - \sum_{f,P=P_L,P_R} \epsilon_{\alpha\beta}^{fP} 2\sqrt{2}G_F(\bar{\nu}_\alpha\gamma^\mu P_L\nu_\beta)(\bar{f}\gamma_\mu P f). \quad (1)$$

Here $P_{L,R}$ are the chirality projectors, $\epsilon_{\alpha\beta}^{fP}$ are the NSI parameters and sum goes over all SM fermions f . Note that the lagrangian (1) contains only operators which do not change flavor of the fermion f . The flavor changing interactions of the type (1) are severely constrained from results on lepton flavor violating and FCNC processes. NC NSI (1) can modify neutrino phenomenology in several ways and these interactions can reveal themselves in scattering processes as well as in neutrino oscillation experiments (see Refs. [4–7] for reviews). Examples of phenomenologically viable models predicting the matter NSI with sizable values of couplings were discussed e.g. in Refs. [8–12].

One of the consequences of the interactions (1) is modification of neutrino propagation in matter. In the presence of NSI the evolution of neutrino having energy E is described by the Hamiltonian

$$H = \frac{1}{2E}U \text{diag}(0, \Delta m_{21}^2, \Delta m_{31}^2)U^\dagger + V_e\epsilon^m, \quad (2)$$

where U is the vacuum Pontecorvo-Maki-Nakagawa-Sakata (PMNS) matrix and $\Delta m_{21}^2, \Delta m_{31}^2$ are differences of the neutrino masses squared. The last term in (2) describes matter effects and it depends on the matter density through $V_e = (-)\sqrt{2}G_F N_e$ for (anti)neutrinos, where N_e is the electron

¹**e-mail:** demidov@ms2.inr.ac.ru

number density. The NSI parameters from the interaction lagrangian (1) enter the Hamiltonian as follows

$$\epsilon^m = \begin{pmatrix} 1 + \epsilon_{ee} & \epsilon_{e\mu} & \epsilon_{e\tau} \\ \epsilon_{e\mu}^* & \epsilon_{\mu\mu} & \epsilon_{\mu\tau} \\ \epsilon_{e\tau}^* & \epsilon_{\mu\tau}^* & \epsilon_{\tau\tau} \end{pmatrix}, \quad (3)$$

where

$$\epsilon_{\alpha\beta} = \sum_{f=e,u,d} (\epsilon_{\alpha\beta}^{fPL} + \epsilon_{\alpha\beta}^{fPR}) \frac{N_f}{N_e}. \quad (4)$$

Here N_f is the number density of the fermion f in matter. In this study we concentrate on neutrino propagation in the Earth and in this case the expression (4) for NSI parameters transforms into

$$\epsilon_{\alpha\beta} \approx \epsilon_{\alpha\beta}^{eV} + 3 \frac{N_u}{N_e} \epsilon_{\alpha\beta}^{uV} + 3 \frac{N_d}{N_e} \epsilon_{\alpha\beta}^{dV}, \quad (5)$$

where $\epsilon_{\alpha\beta}^{fV} \equiv \epsilon_{\alpha\beta}^{fPL} + \epsilon_{\alpha\beta}^{fPR}$. In what follows the notation $\epsilon_{\alpha\beta}$ refers to Eq.(5). In general the parameters $\epsilon_{\alpha\beta}$ are complex-valued numbers. Here we take them real for simplicity (see [13] for recent discussion of the effect of CP violation in NSI).

Atmospheric neutrinos is an important tool to explore neutrino properties and, in particular, to search for new interactions in neutrino sector. The impact of NSI in propagation at experiments with atmospheric neutrinos has been studied extensively (see [14–25] for an incomplete list). Probes with atmospheric neutrinos has been used to constrain the matter NSI in the Earth. Results of experiments with atmospheric neutrinos allow to put rather stringent bounds [26–30] on the parameters $\epsilon_{\alpha\beta}$. Earlier studies of NSI with IceCube data [27, 29, 30] put constraints on the NSI parameters in $\mu\tau$ sector. Preliminary results with the bounds on more generic NSI models were recently reported in [31–33] by IceCube collaboration. In the present study we use the publicly available IceCube DeepCore three-year low energy data sample [34] and perform an independent analysis to constrain the parameters $\epsilon_{\alpha\beta}$. This data sample is very close to what was used by IceCube to measure the neutrino oscillation parameters in Ref. [35]. We perform an analysis of the NSI effect on atmospheric neutrino propagation in the Earth. Information provided by IceCube with the data release [34] and, in particular, results of Monte-Carlo simulation, expected background from atmospheric muons as well as parametrization of estimated instrumental systematic effects, allows one to made a realistic prediction for number of expected events in models with non-zero matter NSI parameters and compare them against the data. As a result we obtain allowed regions for the parameters $\epsilon_{\alpha\beta}$ under certain model assumptions. We compare them with results from other oscillation experiments and discuss impact of systematic uncertainties.

The rest of the paper is organized as follows. In Section 2 we describe methodology used to bound $\epsilon_{\alpha\beta}$ with the IceCube DeepCore three-year data sample. In Section 3 we present our results. Section 4 is reserved for conclusions.

2 Description of the analysis

For the present study we use publicly available three-year data sample [34] in IceCube DeepCore which is referred to as 'Sample B' in² Ref. [37] and which is very close to what was used in the oscillation analysis [35]. This sample contains 40920 events in total which are distributed over

²Another data sample in this release referred to as 'Sample A' was used for measurement of atmospheric tau neutrino appearance [37] and probing for neutrino mass ordering [36].

$8 \times 8 \times 2$ binned histogram. The latter is composed of equally spaced bins in $\log_{10} E^{reco} \in [0.75, 1.75]$, 8 equally spaced bins in $\cos \theta^{reco} \in [-1, 1]$ as well as 2 bins which correspond to the track-like and cascade-like events. Here E^{reco} and θ^{reco} refer to reconstructed values of neutrino energy and zenith angle. We use the public IceCube Monte-Carlo provided along with the data sample to model the detector response and to relate physical values of the energy, zenith angle and type of neutrino with reconstructed characteristics of the events. The simulated neutrino sample released at [34] allows to calculate for each bin i the effective areas $A_i^{\nu_\alpha, t}(E, \cos \theta)$ to be converted with predicted neutrino flux to obtain expected number of events in the bins. The effective areas are obtained as functions of true neutrino energy E in the range from 1 to 1000 GeV, zenith angle θ , neutrino type ν_α and type of neutrino interaction t (CC or NC).

For prediction of the neutrino flux at the detector level we start with the atmospheric neutrino fluxes $\Phi_{\nu_\alpha}^{atm}(E, \theta)$ for $\nu_e, \bar{\nu}_e, \nu_\mu$ and $\bar{\nu}_\mu$ taken from Ref. [38]. To describe propagation of the atmospheric neutrinos in the Earth in presence of NSI one should solve the Schrodinger equation with the Hamiltonian (2) for the case of varying density. In the present analysis we solve it numerically as described in [39, 40] using the algorithm presented in [41]. For calculation of the electron number density in the Earth we use PREM [42]. We fix the following values³ of neutrino oscillation parameters: $\sin^2 \theta_{12} = 0.304$, $\sin^2 \theta_{13} = 0.0217$ and $\Delta m_{21}^2 = 7.53 \cdot 10^{-5} \text{ eV}^2$ and set $\delta_{CP} = 0$. Upon obtaining solution to the Schrodinger equation we calculate the transition probabilities $P_{\nu_\alpha \rightarrow \nu_\beta}(E, \cos \theta)$ to find neutrino of a flavor ν_β at the detector level from neutrino of a flavor ν_α produced in the atmosphere. It is the probability functions $P_{\nu_\alpha \rightarrow \nu_\beta}(E, \cos \theta)$ which depend on the matter NSI parameters $\epsilon_{\alpha\beta}$. The resulting neutrino fluxes at the detector level are then obtained as

$$\Phi_{\nu_\beta}^{det}(E, \cos \theta) = \sum_{\nu_\alpha} \Phi_{\nu_\alpha}^{atm}(E, \cos \theta) P_{\nu_\alpha \rightarrow \nu_\beta}(E, \cos \theta). \quad (6)$$

and the expected number of events in i -th bin can be found as follows

$$n_i^\nu = T \cdot \sum_{t, \nu_\alpha} \int dE d \cos \theta A_i^{\nu_\alpha, t}(E, \cos \theta) \Phi_{\nu_\alpha}^{det}(E, \cos \theta), \quad (7)$$

where T is the lifetime for the data sample under consideration and sum goes over contributions from different neutrino flavors ν_α (including antineutrinos) and interaction types t (CC or NC).

To compare the expected event distribution with the IceCube DeepCore data we take into account systematic uncertainties and our procedure includes a set of relevant nuisance parameters η_j . They correspond to overall normalization of atmospheric neutrino flux with no prior, the spectral index of the atmospheric neutrino flux with the nominal value $\gamma = -2.66$ and a prior $\sigma_\gamma = 0.1$, relative normalizations of $\nu_e, \bar{\nu}_e$ events and NC events with an uncertainty 20%. Also we include additional corrections to the atmospheric neutrino flux at production to take into account uncertainties in the hadron production in atmosphere. This corrections as functions of neutrino energy and zenith angle have been chosen to reproduce the uncertainties estimated in Ref. [47] similar to how it was done in [48]. Also we take into account uncertainty related to the neutrino nucleon cross section with baryon resonance production which is important for low energy part of the neutrino sample. For that we introduce an additional nuisance parameter for the contribution from such type of the events with 40% uncertainty which is close to what was found in [48]. As discussed in [35] uncertainties on

³We note that analysis of solar neutrino propagation revealed [43] that models with NSI allow for so-called LMA-D solution for the oscillation parameters for which $\sin^2 \theta_{12} > 0.5$. In this study we do not consider this possibility because, on the one hand, the impact of $\sin^2 \theta_{12}$ on the results of our analysis is very mild and, on the other, recent studies (see e.g. [44–46]) showed that the LMA-D scenario is disfavored by experimental data.

the DIS cross section have negligible impact on the results. We include in the analysis the template for the background of atmospheric muons with corresponding uncorrelated error $\sigma_{\nu,\mu atm}^{uncor}$ provided by IceCube for this data sample [34]. Normalization of the background is taken as a nuisance parameter with no prior. Finally, we account for instrumental systematic uncertainties related to the optical efficiencies of DOMs and relevant properties of the ice. These uncertainties are included in our analysis as described in [34]. In summary, our implementation of the systematic uncertainties is very close to how it was done in the original oscillation analysis [35]. We will discuss the impact of the most important systematic errors in the next Section.

Let us note, that in general interactions of the type (1) result in changes of the NC neutrino-nucleon cross section and thus can modify expected number of events. However, this effect is very model dependent. Not only it depends on other combinations of the parameters $\epsilon_{\alpha\beta}^{fP}$ than those in Eq. (5), but it is also affected by microscopic model behind the effective lagrangian (1) and the resulting cross section will be different for models with light and heavy mediators. In the present analysis we conservatively do not take into account the impact of NSI on the modification on the NC neutrino-nucleon cross sections.

To obtain bounds on the parameters of non-standard neutrino interactions we define (c.f. Eq.(2) in [35])

$$\chi^2 = \sum_i \frac{(n_i^\nu + n_i^{\mu atm} - n_i^{data})^2}{(\sigma_i^{data})^2 + (\sigma_{\nu,\mu atm,i}^{uncor})^2} + \sum_j \frac{(\eta_j - \hat{\eta}_j)^2}{\sigma_{\eta_j}^2}, \quad (8)$$

where n_i^ν ($n_i^{\mu atm}$) is the expected number of events from atmospheric neutrinos (muons), n_i^{data} is the number of data events in the i -th bin, $\sigma_i^{data} = \sqrt{n_i^{data}}$, and the first sum goes over all bins in the data sample. The second term accounts for contribution from the nuisance parameters η_j , given their default values $\hat{\eta}_j$ and uncertainties σ_{η_j} . We fix $\sin^2 \theta_{12}$, $\sin^2 \theta_{13}$ and Δm_{21}^2 as described above. We checked that the uncertainties in their values produce negligible effect on the final results. Also we assume $\delta_{CP} = 0$. Other neutrino oscillation parameters, $\sin^2 \theta_{23}$ and Δm_{31}^2 , are not fixed to any *a priori* value but were determined from the analysis itself in most part of the study. As a consistency check we reproduce confidence regions for $\sin^2 \theta_{23}$ and Δm_{31}^2 from the IceCube DeepCore data sample assuming $\epsilon_{\alpha\beta} = 0$. In particular, we find for the case of normal mass ordering $\sin^2 \theta_{23} = 0.52_{-0.08}^{+0.07}$, $\Delta m_{32}^2 = 2.29_{-0.15}^{+0.16}$ eV² which is very close to those intervals obtained in Ref. [35]. In our analysis with non-vanishing matter NSI parameters we consider $\sin^2 \theta_{23}$ and Δm_{31}^2 as nuisance parameters with no prior unless stated otherwise. In Section 3 we discuss how the bounds on $\epsilon_{\alpha\beta}$ are robust if $\sin^2 \theta_{23}$ and Δm_{31}^2 are fixed in the analysis.

The IceCube DeepCore low energy data sample of the atmospheric neutrinos [34] contains (contrary to the earlier IceCube DeepCore oscillation analyses [49]) not only track-like but also cascade-like events which results mainly from CC interactions of ν_μ and ν_e (see Fig. 1 in Ref. [35]). This makes the data sample sensitive not only to changes in the muon neutrino flux but also to modification in the flux of electron neutrinos. Most of the theoretical studies discuss impact of the NSI in propagation mainly on the muon neutrino flux $\Phi_{\nu_\mu}^{det}$. This is mostly sufficient for the models with non-zero values of the corresponding parameters in $\mu\tau$ sector where the NSI effect on the electron neutrino flux is very mild given current bounds on the NSI parameters. However, this is not the case for models with non-zero $\epsilon_{e\tau}$ or $\epsilon_{e\mu}$. For illustration, in Figs. 1 and 2 we show oscillograms for $\Delta P_{\mu\mu}$ and $\Delta P_{\mu e}$ which are the differences between the transition probabilities with and without NSI, i.e. $\Delta P_{\alpha\beta} = P_{\nu_\alpha \rightarrow \nu_\beta}^{NSI} - P_{\nu_\alpha \rightarrow \nu_\beta}^{noNSI}$ for neutrinos. Fig. 1 and 2 correspond to $\epsilon_{e\tau} = 0.3$ and $\epsilon_{e\mu} = 0.3$, respectively. Right panels on both Figures correspond to $\Delta P_{\mu\mu}$ while left are reserved for $\Delta P_{\mu e}$. We observe that the off-diagonal matter NSI involving electron neutrinos may considerably modify not only the fluxes of muon neutrinos but also that of electron neutrinos. Note that the effect of non-zero

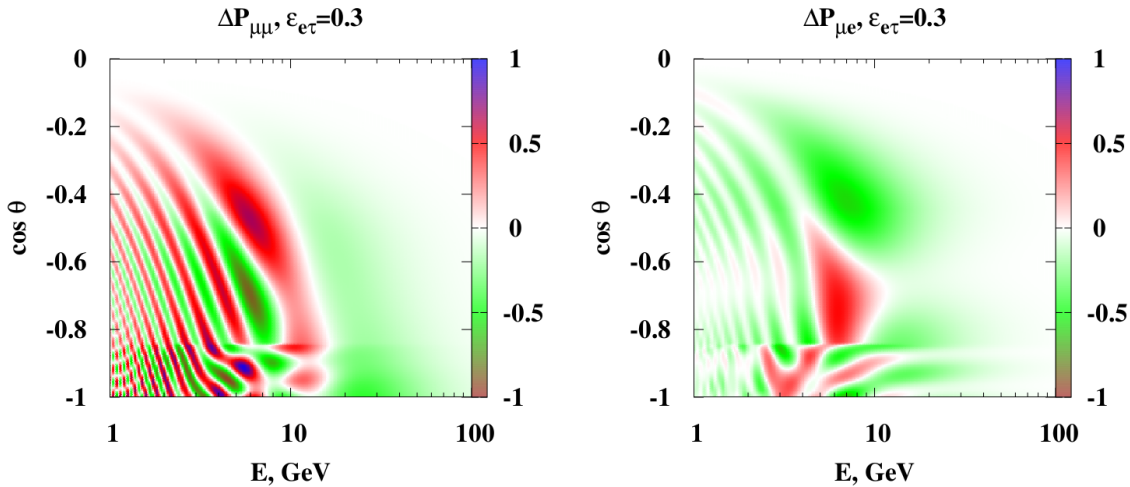


Figure 1: Differences between probabilities $\Delta P_{\mu\mu} \equiv P_{\nu_\mu \rightarrow \nu_\mu}^{NSI} - P_{\nu_\mu \rightarrow \nu_\mu}^{noNSI}$ (left panel) and $\Delta P_{\mu e} \equiv P_{\nu_\mu \rightarrow \nu_e}^{NSI} - P_{\nu_\mu \rightarrow \nu_e}^{noNSI}$ (right panel) shown in color as functions of E and $\cos\theta$. The probabilities are calculated with $\epsilon^{e\tau} = 0.3$ assuming $\sin^2\theta_{23} = 0.51$ and $\Delta m_{31}^2 = 2.5 \times 10^{-3} \text{ eV}^2$.

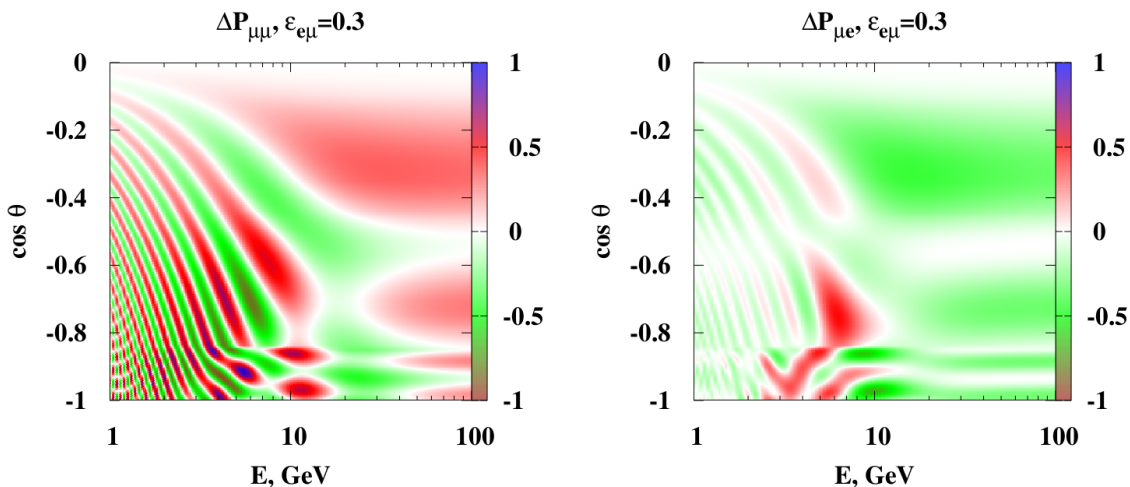


Figure 2: The same as in Fig. 1 but with $\epsilon_{e\mu} = 0.3$.

$\epsilon_{e\tau}$ decreases with increase of neutrino energy but this is not the case for $\epsilon_{e\mu}$. Thus we expect that IceCube data for neutrinos at high energies will be also sensitive to the parameter $\epsilon_{e\mu}$.

3 Results

In this Section we present results on the allowed regions for several matter NSI parameters $\epsilon_{\alpha\beta}$ from the analysis of the low energy three-year IceCube DeepCore data sample [34]. In this study we limit ourselves to a constrained analysis in the matter NSI parameter space assuming only some of $\epsilon_{\alpha\beta}$ to be non-zero. As neutrino oscillation probabilities depend on differences between the diagonal elements $\epsilon_{ee} - \epsilon_{\mu\mu}$ and $\epsilon_{\tau\tau} - \epsilon_{\mu\mu}$ we fix $\epsilon_{\mu\mu} = 0$ in what follows.

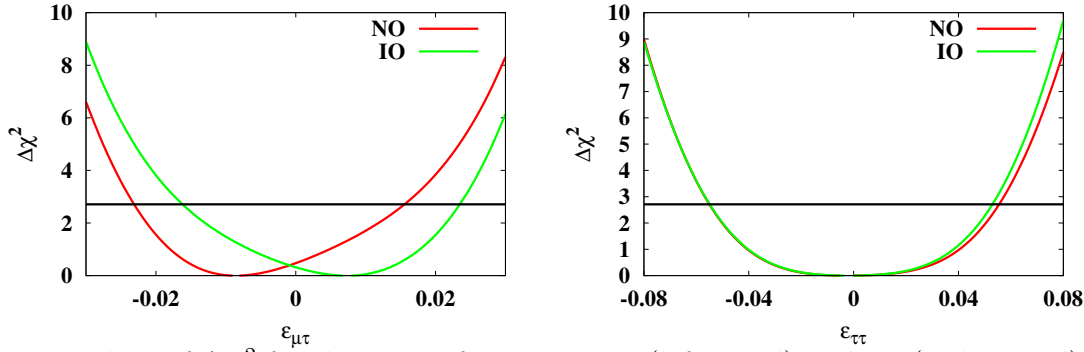


Figure 3: Values of $\Delta\chi^2$ for the cases of non-zero $\epsilon_{\mu\tau}$ (left panel) and $\epsilon_{\tau\tau}$ (right panel). Other matter NSI parameters except for $\epsilon_{\mu\tau}$ (left panel) and $\epsilon_{\tau\tau}$ (right panel) are set to zero. Red (dark gray) and green (light gray) lines correspond to normal and inverted neutrino mass hierarchy, respectively.

Let us start with the $\mu\tau$ sector where the NSI parameters, $\epsilon_{\mu\tau}$ and $\epsilon' \equiv \epsilon_{\tau\tau} - \epsilon_{\mu\mu}$, are known to be severely constrained from experiments with atmospheric neutrinos [27, 29, 30]. Firstly, we take a single non-zero matter NSI parameter, $\epsilon_{\mu\tau}$ or $\epsilon_{\tau\tau}$, at a time and perform minimization of χ^2 given by Eq. (8) with respect to all other variables (including Δm_{31}^2 , $\sin^2 \theta_{23}$ and other nuisance parameters discussed in previous Section). We consider the cases of normal (NO) and inverted (IO) neutrino mass ordering independently. The results for $\Delta\chi^2 \equiv \chi^2 - \chi_{min}^2$, where χ_{min}^2 is an absolute minimum of χ^2 for each case, are shown in Fig. 3 for non-zero $\epsilon_{\mu\tau}$ (left panel) and $\epsilon_{\tau\tau}$ (right panel). We find the following single parameter allowed ranges at 90% C.L.

$$-0.023 < \epsilon_{\mu\tau} < 0.016 \text{ (NO)}, \quad -0.016 < \epsilon_{\mu\tau} < 0.023 \text{ (IO)}, \quad (9)$$

$$-0.055 < \epsilon_{\tau\tau} < 0.056 \text{ (NO)}, \quad -0.055 < \epsilon_{\tau\tau} < 0.053 \text{ (IO)}. \quad (10)$$

Note that the obtained regions for $\epsilon_{\mu\tau}$ are consistent⁴ with those $-0.020 < \epsilon_{\mu\tau} < 0.024$ (NO) obtained by IceCube collaboration [30] in a similar single parameter analysis using three years of their data with upward going track events selection. The regions (9), (10) are also close to the preliminary IceCube bounds $|\epsilon_{\mu\tau}| \lesssim 0.17$ and $|\epsilon_{\tau\tau}| \lesssim 0.04$ (NO) from an analysis of DeepCore data reported⁵ in [33].

Next, we consider the NSI models in which both parameters in the $\mu\tau$ sector, i.e. $\epsilon_{\mu\tau}$ and $\epsilon_{\tau\tau}$, are not equal to zero. Corresponding allowed regions on $(\epsilon_{\mu\tau}, \epsilon_{\tau\tau})$ plane are presented in Fig. 4 for NO (left panel) and IO (right panel). After marginalization with respect to each of these parameters we obtain the following allowed ranges at 90% C.L.

$$-0.027 < \epsilon_{\mu\tau} < 0.022 \text{ (NO)}, \quad -0.022 < \epsilon_{\mu\tau} < 0.027 \text{ (IO)}, \quad (11)$$

$$-0.063 < \epsilon_{\tau\tau} < 0.064 \text{ (NO)}, \quad -0.064 < \epsilon_{\tau\tau} < 0.061 \text{ (IO)}, \quad (12)$$

which are only slightly wider than those found in the single parameter analysis and shown in (9),(10). The marginalized bounds on $\epsilon_{\mu\tau}$ are weaker than the allowed range $-0.018 < \epsilon_{\mu\tau} < 0.016$ (NO), 90% C.I. obtained in Ref. [29] from the analysis of a one year high energy IceCube data sample [50] and than the earlier bound $-0.018 < \epsilon_{\mu\tau} < 0.017$ (NO) at 90% C.L. obtained in Ref. [27] using the data from 79-string IceCube configuration and DeepCore. At the same time the marginalized bounds (12)

⁴With our convention (4) the values of $\epsilon_{\alpha\beta}$ differ by a factor of $r \equiv N_d/N_e \approx 3$ from those used e.g. in [26, 29, 30].

⁵Note that the analysis [33] assumes presence of the complex phases in the flavour changing NSI parameters. For consistency, here we cite preliminary bounds for real valued parameters.

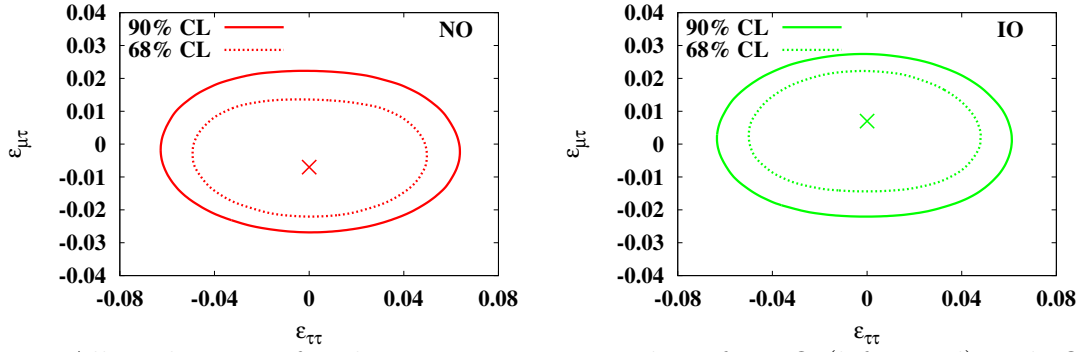


Figure 4: Allowed regions for the parameters $\epsilon_{\mu\tau}$ and $\epsilon_{\tau\tau}$ for NO (left panel) and IO (right panel). Other parameters $\epsilon_{\alpha\beta}$ of the matter NSI are set to zero.

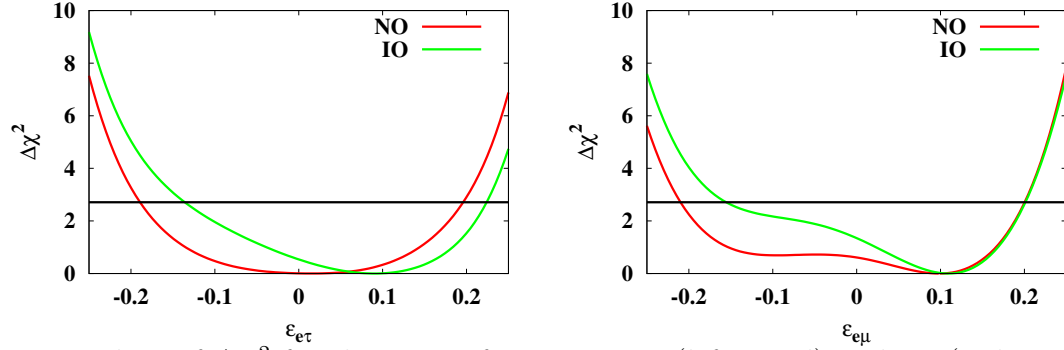


Figure 5: Values of $\Delta\chi^2$ for the cases of non-zero $\epsilon_{e\tau}$ (left panel) and $\epsilon_{e\mu}$ (right panel). Other NSI parameters except for $\epsilon_{e\tau}$ (left panel) and $\epsilon_{e\mu}$ (right panel) are set to zero. Red (dark gray) and green (light gray) lines correspond to NO and IO, respectively.

on the parameter $\epsilon' \equiv \epsilon_{\tau\tau}$ are somewhat better than the allowed range $-0.11 < \epsilon' < 0.09$ at 90% C.L. from Ref. [27] and the constraint $|\epsilon'| < 0.15$ obtained by Super-Kamiokande experiment [26]. Comparable bound on ϵ' was obtained in Ref. [29] from a combination of high energy IceCube data and Super-Kamiokande results. Let us note that the effect of ϵ' on neutrino propagation decreases with neutrino energy (see e.g. [27]) and thus to probe this parameter one should rely on low energy part of the atmospheric neutrino spectrum.

Now let us turn to the NSI models with non-zero parameters involving electron neutrinos. In Fig. 5 we show $\Delta\chi^2$ for NSI models with non-zero flavor changing parameters $\epsilon_{e\tau}$ (left panel) and $\epsilon_{e\mu}$ (right panel) taking a single non-zero NSI parameter at a time. Corresponding allowed regions at 90% C.L. read

$$-0.21 < \epsilon_{e\mu} < 0.20 \text{ (NO)}, \quad -0.16 < \epsilon_{e\mu} < 0.20 \text{ (IO)}, \quad (13)$$

$$-0.19 < \epsilon_{e\tau} < 0.20 \text{ (NO)}, \quad -0.14 < \epsilon_{e\tau} < 0.22 \text{ (IO)}. \quad (14)$$

The allowed single parameter bounds for $\epsilon_{e\mu}$ and $\epsilon_{e\tau}$ are consistent with the preliminary results $|\epsilon_{e\mu}| \lesssim 0.16$ and $|\epsilon_{e\tau}| \lesssim 0.2$ (NO) reported by IceCube [33]. Note that based on the behaviour of $\Delta P_{\mu\mu}$ and $\Delta P_{\mu e}$ shown in Fig. 2 one can expect an improvement in the allowed ranges on $\epsilon_{e\mu}$ with data on atmospheric neutrino at high energies. It is well known that the effect of $\epsilon_{e\tau}$ on neutrino transition probabilities strongly depends on the values of other matter NSI parameters. Following the analysis [26] and earlier studies [15, 17] let us consider the NSI models with non-zero parameters in $e\tau$ sector, i.e. $\epsilon_{ee}, \epsilon_{e\tau}$ and $\epsilon_{\tau\tau}$. In Fig. 6 we show allowed regions for $\epsilon_{e\tau}$ and $\epsilon_{\tau\tau}$

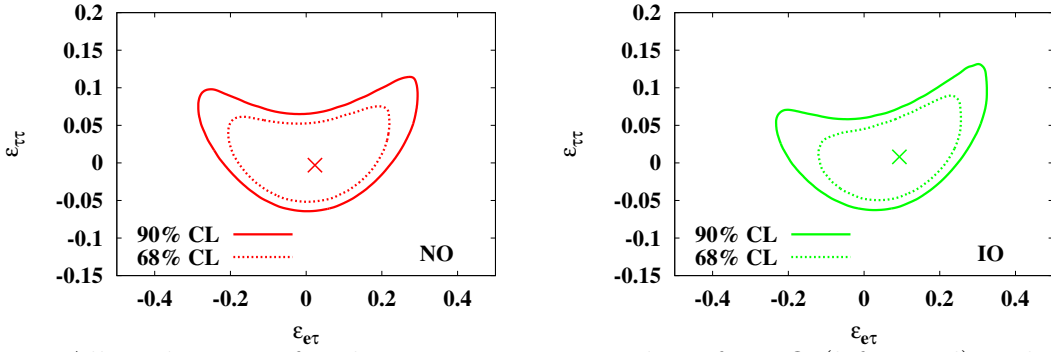


Figure 6: Allowed regions for the parameters $\epsilon_{e\tau}$ and $\epsilon_{\tau\tau}$ for NO (left panel) and IO (right panel). Other parameters of the matter NSI including ϵ_{ee} are set to zero.

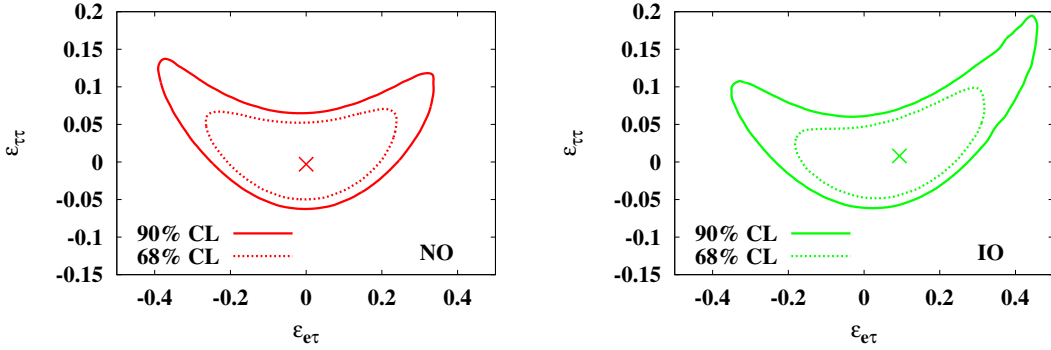


Figure 7: The same as in Fig. 6 but for $\epsilon_{ee} = 0.2$.

within these models assuming $\epsilon_{ee} = 0$. The parabolic form of the allowed region comes from the approximate relation $\epsilon_{\tau\tau} \sim \frac{|\epsilon_{e\tau}|^2}{1+\epsilon_{ee}}$, which should be satisfied for consistency with high energy part of the atmospheric neutrino spectrum, see [15, 17]. Similar allowed regions from preliminary analysis of tree-year DeepCore data were presented in [31]. The sensitivity of the considered dataset to ϵ_{ee} is relatively weak, but still its non-zero value may affect the bounds on $\epsilon_{e\tau}$ and $\epsilon_{\tau\tau}$ in this class of NSI models through the above relation. As an illustration, in Figs. 7 and 8 are shown the allowed regions in $(\epsilon_{\tau\tau}, \epsilon_{e\tau})$ plane assuming $\epsilon_{ee} = 0.2$ and -0.2 , respectively. We see the dependence of the bounds for $\epsilon_{e\tau}$ on the assumption about the value of ϵ_{ee} . The same is valid for allowed regions for $\epsilon_{\tau\tau}$ which can be considerably modified as compared to those given by Eq. (12) obtained for the NSI models with other $\epsilon_{\alpha\beta} = 0$. The found allowed regions for $\epsilon_{e\tau}$ and $\epsilon_{\tau\tau}$ are compatible to the latest constraints on these parameters obtained with the Super-Kamiokande data in Ref. [28] using somewhat different ansatz for the parameter space.

Finally we study impact of different nuisance parameters discussed in Section 2 on our results. Firstly, in Fig. 9 we present $\Delta\chi^2$ obtained in the single-parameter analyses (for NSI models with non-zero $\epsilon_{\mu\tau}$, $\epsilon_{\tau\tau}$, $\epsilon_{e\tau}$ or $\epsilon_{e\mu}$ and assuming normal neutrino mass ordering) for the case with all systematic uncertainties included (which is our default analysis) in comparison with those obtained with (a) fixed nuisance parameters related directly to the uncertainties in atmospheric neutrino flux, i.e. spectral index and uncertainties in the hadron production in atmosphere, (b) fixed nuisance parameters related to the experimental systematic uncertainties and (c) fixed nuisance parameters which determine normalizations of different contributions to expected number of events including those related to the neutrino nucleon cross section and atmospheric muon background. For illustration we present results for the case of normal mass ordering. One observes that the most important systematic uncertainties

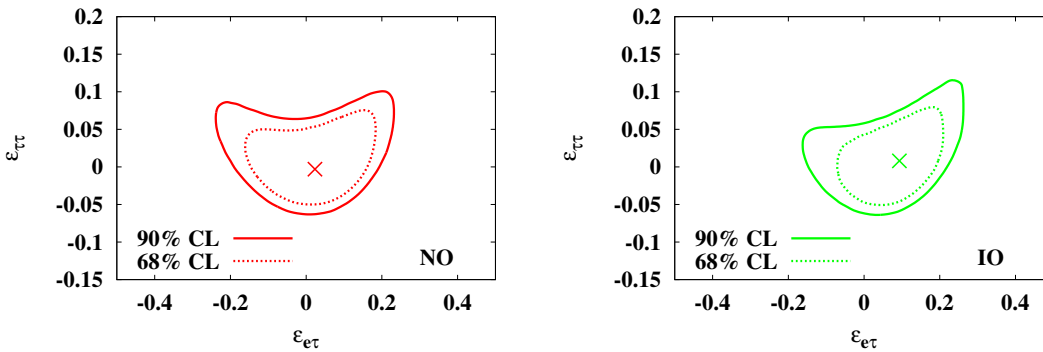


Figure 8: The same as in Fig. 6 but for $\epsilon_{ee} = -0.2$.

are the experimental ones and those related to atmospheric neutrino flux, specifically for the NSI models with non-zero $\epsilon_{e\tau}$ and $\epsilon_{\mu\tau}$. We also study impact of neutrino oscillation parameters, i.e. $\sin^2 \theta_{23}$ and Δm_{31}^2 . As an example, we fix them to their optimal values without NSI for the case of normal mass ordering (see Section 2). Corresponding allowed ranges for $\epsilon_{\mu\tau}, \epsilon_{\tau\tau}, \epsilon_{e\tau}, \epsilon_{e\mu}$ (a single non-zero NSI parameter at a time) becomes

$$-0.19 < \epsilon_{\mu\tau} < 0.13, \quad -0.052 < \epsilon_{\tau\tau} < 0.051, \quad (15)$$

$$-0.17 < \epsilon_{e\tau} < 0.16, \quad -0.20 < \epsilon_{e\mu} < 0.18. \quad (16)$$

By comparison with (9),(10) and (13),(14) we see that the oscillation parameters affect very little these bounds.

4 Conclusions

Let us summarize results of our study. Here we used the three-year IceCube DeepCore data sample [34] of low energy atmospheric neutrinos to constrain the parameters of non-standard neutrino interactions in propagation. This data sample contains track-like as well as cascade-like events which makes it sensitive not mainly to muon but also to electron neutrino flux at the detector level. Using this dataset we found the bounds on several $\epsilon_{\alpha\beta}$ under different model assumptions. In particular, we presented allowed regions for the matter NSI parameters, assuming 1) single non-zero parameter at a time, 2) non-zero parameters in $\mu\tau$ sector and 3) non-zero $\epsilon_{e\tau}$ and $\epsilon_{\tau\tau}$ for several fixed values of ϵ_{ee} . The bounds on $\epsilon_{\mu\tau}$ and $\epsilon_{\tau\tau}$ were found to be close to those [27–30] extracted from different data samples of the IceCube/DeepCore as well as from Super-Kamiokande results. Obtained single-parameter bounds on $\epsilon_{\mu\tau}, \epsilon_{\tau\tau}, \epsilon_{e\tau}$ and $\epsilon_{e\mu}$ are consistent with the preliminary IceCube results [31–33] from a similar analysis of three-year DeepCore data. We studied the impact of different sources of systematic uncertainties and found that the obtained bounds are mainly stable with respect to the nuisance parameters of the analysis. The main errors in the bounds results from uncertainties in the atmospheric neutrino flux and from experimental uncertainties. They are specifically important for single parameter bounds on $\epsilon_{e\tau}$ and $\epsilon_{e\mu}$. Note that from energy dependence of neutrino transition probabilities we can expect an improvement in the bound on $\epsilon_{e\mu}$ using studies with high energy part of atmospheric neutrino spectrum.

In the main text we made a comparison mainly with the results obtained from oscillation experiments with atmospheric neutrinos. The obtained bounds on $\epsilon_{\mu\tau}, \epsilon_{\tau\tau}, \epsilon_{e\tau}$ and $\epsilon_{e\mu}$ are also consistent with the results of global analysis of neutrino oscillation experiments [51] (see also [22, 52, 53] for earlier studies) obtained under assumptions that the matter NSI are given by neutrino interactions with

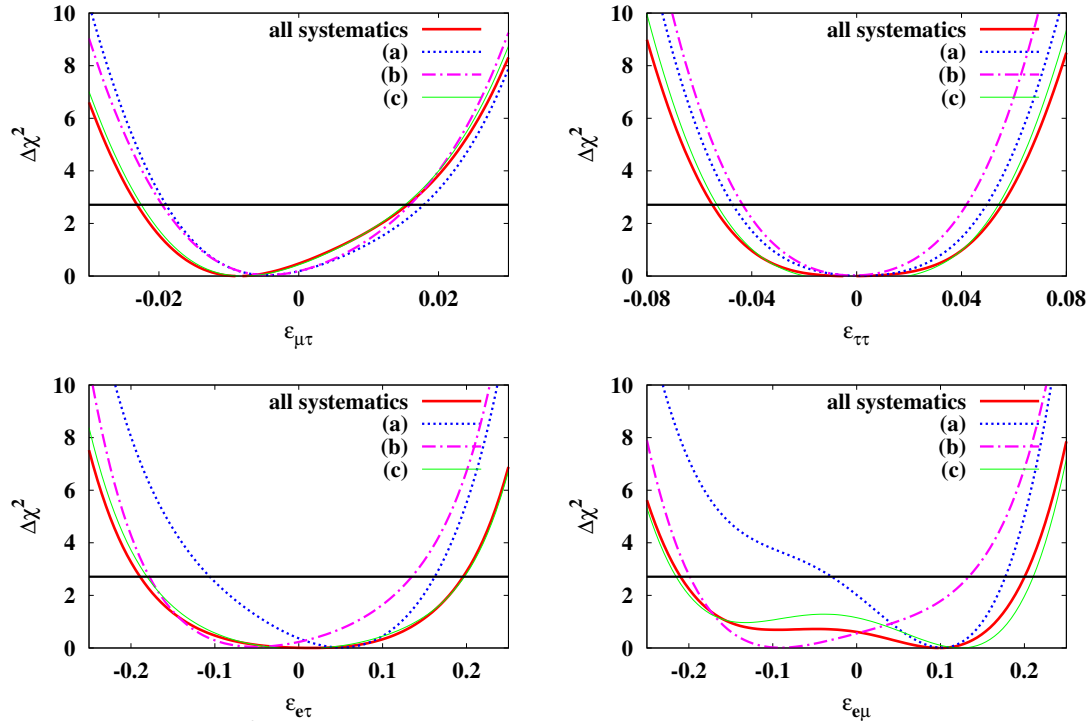


Figure 9: Values of $\Delta\chi^2$ (NO) for the NSI models with non-zero values of $\epsilon_{\mu\tau}$ (upper left), $\epsilon_{\tau\tau}$ (upper right), $\epsilon_{e\tau}$ (lower left) and $\epsilon_{e\mu}$ (lower right) obtained in the analyses with all systematic uncertainties included (red thick solid line) in comparison with those obtained with (a) fixed nuisance parameters related to atmospheric neutrino flux (blue dotted line), (b) fixed nuisance parameters related to the experimental uncertainties (magenta dashed-dotted line) and (c) fixed nuisance parameters related to normalization of different contributions to expected number of events (green thin solid line).

quarks only and that their flavour structure is independent of the quark flavour. Further insight on possible strength of NSI can be obtained by combining with the results of scattering experiments [46, 54] (see also [55, 56]). Here we were interested in the impact of the low energy IceCube DeepCore data [34] solely and leaved a combined analysis for future study.

I am grateful to Philipp Eller for helpful correspondence. The work was supported by the RSF grant 17-12-01547.

References

- [1] M. Tanabashi *et al.* [Particle Data Group], Phys. Rev. D **98** (2018) no.3, 030001.
- [2] L. Wolfenstein, Phys. Rev. D **17** (1978) 2369.
- [3] M. M. Guzzo, A. Masiero and S. T. Petcov, Phys. Lett. B **260** (1991) 154.
- [4] T. Ohlsson, Rept. Prog. Phys. **76** (2013) 044201 [arXiv:1209.2710 [hep-ph]].
- [5] O. G. Miranda and H. Nunokawa, New J. Phys. **17** (2015) no.9, 095002 [arXiv:1505.06254 [hep-ph]].
- [6] Y. Farzan and M. Tortola, Front. in Phys. **6** (2018) 10 [arXiv:1710.09360 [hep-ph]].

- [7] P. S. Bhupal Dev *et al.*, “Neutrino Non-Standard Interactions: A Status Report,” arXiv:1907.00991 [hep-ph].
- [8] Y. Farzan, Phys. Lett. B **748** (2015) 311 doi:10.1016/j.physletb.2015.07.015 [arXiv:1505.06906 [hep-ph]].
- [9] Y. Farzan and I. M. Shoemaker, JHEP **1607** (2016) 033 doi:10.1007/JHEP07(2016)033 [arXiv:1512.09147 [hep-ph]].
- [10] Y. Farzan and J. Heeck, Phys. Rev. D **94** (2016) no.5, 053010 doi:10.1103/PhysRevD.94.053010 [arXiv:1607.07616 [hep-ph]].
- [11] Y. Farzan, “Viable models for large non-standard neutrino interactions,” arXiv:1612.04971 [hep-ph].
- [12] K. S. Babu, P. S. B. Dev, S. Jana and A. Thapa, “Non-Standard Interactions in Radiative Neutrino Mass Models,” arXiv:1907.09498 [hep-ph].
- [13] I. Esteban, M. C. Gonzalez-Garcia and M. Maltoni, JHEP **1906** (2019) 055 [arXiv:1905.05203 [hep-ph]].
- [14] M. C. Gonzalez-Garcia and M. Maltoni, Phys. Rev. D **70** (2004) 033010 [hep-ph/0404085].
- [15] A. Friedland, C. Lunardini and M. Maltoni, Phys. Rev. D **70** (2004) 111301 [hep-ph/0408264].
- [16] M. Blennow, T. Ohlsson and W. Winter, Eur. Phys. J. C **49** (2007) 1023 [hep-ph/0508175].
- [17] A. Friedland and C. Lunardini, Phys. Rev. D **72** (2005) 053009 [hep-ph/0506143].
- [18] M. C. Gonzalez-Garcia, F. Halzen and M. Maltoni, Phys. Rev. D **71** (2005) 093010 [hep-ph/0502223].
- [19] W. A. Mann, D. Cherdack, W. Musial and T. Kafka, Phys. Rev. D **82** (2010) 113010 [arXiv:1006.5720 [hep-ph]].
- [20] T. Ohlsson, H. Zhang and S. Zhou, Phys. Rev. D **88** (2013) no.1, 013001 doi:10.1103/PhysRevD.88.013001 [arXiv:1303.6130 [hep-ph]].
- [21] S. Choubey and T. Ohlsson, Phys. Lett. B **739** (2014) 357 [arXiv:1410.0410 [hep-ph]].
- [22] M. C. Gonzalez-Garcia, M. Maltoni and J. Salvado, JHEP **1105** (2011) 075 [arXiv:1103.4365 [hep-ph]].
- [23] I. Mocioiu and W. Wright, Nucl. Phys. B **893** (2015) 376 [arXiv:1410.6193 [hep-ph]].
- [24] A. Chatterjee, P. Mehta, D. Choudhury and R. Gandhi, Phys. Rev. D **93** (2016) no.9, 093017 [arXiv:1409.8472 [hep-ph]].
- [25] S. Fukasawa and O. Yasuda, Nucl. Phys. B **914** (2017) 99 [arXiv:1608.05897 [hep-ph]].
- [26] G. Mitsuka *et al.* [Super-Kamiokande Collaboration], Phys. Rev. D **84** (2011) 113008 [arXiv:1109.1889 [hep-ex]].
- [27] A. Esmaili and A. Y. Smirnov, JHEP **1306** (2013) 026 [arXiv:1304.1042 [hep-ph]].

- [28] S. Fukasawa and O. Yasuda, *Adv. High Energy Phys.* **2015** (2015) 820941 [arXiv:1503.08056 [hep-ph]].
- [29] J. Salvado, O. Mena, S. Palomares-Ruiz and N. Rius, *JHEP* **1701** (2017) 141 [arXiv:1609.03450 [hep-ph]].
- [30] M. G. Aartsen *et al.* [IceCube Collaboration], *Phys. Rev. D* **97** (2018) no.7, 072009 [arXiv:1709.07079 [hep-ex]].
- [31] T. Ehrhardt (for the IceCube Collaboration), “Search for NSI with IceCube DeepCore”, Poster presented at the Advanced Workshop on Physics of Atmospheric Neutrinos - PANE 2018, May 28 – June 1, 2018, Trieste (Italy).
- [32] C. de los Heros, “Particle Physics with IceCube”, talk at the XVIII International Workshop on Neutrino Telescopes, Venice, March 18-22, 2019.
- [33] T. Ehrhardt (for the IceCube Collaboration), “Search for NSI in neutrino propagation with IceCube DeepCore”, talk at the 4th Uppsala workshop on Particle Physics with Neutrino Telescopes (PPNT19), Uppsala, October 7-9, 2019.
- [34] IceCube Collaboration (2019): Three-year high-statistics neutrino oscillation samples. DOI:10.21234/ac23-ra43 , https://icecube.wisc.edu/science/data/highstats_nuosc_3y
- [35] M. G. Aartsen *et al.* [IceCube Collaboration], *Phys. Rev. Lett.* **120** (2018) no.7, 071801 [arXiv:1707.07081 [hep-ex]].
- [36] M. G. Aartsen *et al.* [IceCube Collaboration], arXiv:1902.07771 [hep-ex].
- [37] M. G. Aartsen *et al.* [IceCube Collaboration], *Phys. Rev. D* **99** (2019) no.3, 032007 [arXiv:1901.05366 [hep-ex]].
- [38] M. Honda, M. Sajjad Athar, T. Kajita, K. Kasahara and S. Midorikawa, *Phys. Rev. D* **92** (2015) no.2, 023004 [arXiv:1502.03916 [astro-ph.HE]].
- [39] M. M. Boliev, S. V. Demidov, S. P. Mikheyev and O. V. Suvorova, *JCAP* **1309** (2013) 019 [arXiv:1301.1138 [astro-ph.HE]].
- [40] S. V. Demidov, *JCAP* **1802** (2018) 001 [arXiv:1711.00911 [hep-ph]].
- [41] T. Ohlsson and H. Snellman, *J. Math. Phys.* **41** (2000) 2768 Erratum: [*J. Math. Phys.* **42** (2001) 2345] [hep-ph/9910546].
- [42] A. M. Dziewonski and D. L. Anderson, *Phys. Earth Planet. Interiors* **25** (1981) 297.
- [43] O. G. Miranda, M. A. Tortola and J. W. F. Valle, *JHEP* **0610** (2006) 008 [hep-ph/0406280].
- [44] P. Coloma, M. C. Gonzalez-Garcia, M. Maltoni and T. Schwetz, *Phys. Rev. D* **96** (2017) no.11, 115007 doi:10.1103/PhysRevD.96.115007 [arXiv:1708.02899 [hep-ph]].
- [45] C. Giunti, “General COHERENT Constraints on Neutrino Non-Standard Interactions,” arXiv:1909.00466 [hep-ph].

- [46] P. Coloma, I. Esteban, M. C. Gonzalez-Garcia and M. Maltoni, JHEP **2002** (2020) 023 doi:10.1007/JHEP02(2020)023 [arXiv:1911.09109 [hep-ph]].
- [47] G. D. Barr, T. K. Gaisser, S. Robbins and T. Stanev, Phys. Rev. D **74** (2006) 094009 [astro-ph/0611266].
- [48] A. Terliuk, Ph.D. thesis, “Measurement of atmospheric neutrino oscillations and search for sterile neutrino mixing with IceCube DeepCore,”
- [49] M. G. Aartsen *et al.* [IceCube Collaboration], Phys. Rev. D **91** (2015) no.7, 072004 [arXiv:1410.7227 [hep-ex]].
- [50] M. G. Aartsen *et al.* [IceCube Collaboration], Phys. Rev. Lett. **117** (2016) no.7, 071801 [arXiv:1605.01990 [hep-ex]].
- [51] I. Esteban, M. C. Gonzalez-Garcia, M. Maltoni, I. Martinez-Soler and J. Salvado, JHEP **1808** (2018) 180 [arXiv:1805.04530 [hep-ph]].
- [52] M. C. Gonzalez-Garcia and M. Maltoni, JHEP **1309** (2013) 152 [arXiv:1307.3092 [hep-ph]].
- [53] M. C. Gonzalez-Garcia, M. Maltoni and T. Schwetz, Nucl. Phys. B **908** (2016) 199 [arXiv:1512.06856 [hep-ph]].
- [54] P. Coloma, P. B. Denton, M. C. Gonzalez-Garcia, M. Maltoni and T. Schwetz, JHEP **1704** (2017) 116 [arXiv:1701.04828 [hep-ph]].
- [55] J. Barranco, O. G. Miranda, C. A. Moura and J. W. F. Valle, Phys. Rev. D **77** (2008) 093014 [arXiv:0711.0698 [hep-ph]].
- [56] C. Biggio, M. Blennow and E. Fernandez-Martinez, JHEP **0908** (2009) 090 [arXiv:0907.0097 [hep-ph]].